



The role of meteorological conditions and pollution control strategies in reducing air pollution in Beijing during APEC 2014 and Victory Parade 2015

Pengfei Liang¹, Tong Zhu¹, Yanhua Fang¹, Yingruo Li^{1,2}, Yiqun Han¹, Yusheng Wu¹, Min Hu¹, and Junxia Wang¹

¹SKL-ESPC and BIC-ESAT, College of Environmental Sciences and Engineering, Peking University, Beijing, 100871, China

²Environmental Meteorology Forecast Center of Beijing-Tianjin-Hebei, China Meteorological Administration, Beijing, 100089, China

Correspondence to: Tong Zhu (tzh@pku.edu.cn)

Received: 14 May 2017 – Discussion started: 29 May 2017

Revised: 28 September 2017 – Accepted: 11 October 2017 – Published: 23 November 2017

Abstract. To control severe air pollution in China, comprehensive pollution control strategies have been implemented throughout the country in recent years. To evaluate the effectiveness of these strategies, the influence of meteorological conditions on levels of air pollution needs to be determined. Using the intensive air pollution control strategies implemented during the Asia-Pacific Economic Cooperation Forum in 2014 (APEC 2014) and the 2015 China Victory Day Parade (Victory Parade 2015) as examples, we estimated the role of meteorological conditions and pollution control strategies in reducing air pollution levels in Beijing. Atmospheric particulate matter of aerodynamic diameter $\leq 2.5 \mu\text{m}$ ($\text{PM}_{2.5}$) samples were collected and gaseous pollutants (SO_2 , NO , NO_x , and O_3) were measured online at a site in Peking University (PKU). To determine the influence of meteorological conditions on the levels of air pollution, we first compared the air pollutant concentrations during days with stable meteorological conditions. However, there were few days with stable meteorological conditions during the Victory Parade. As such, we were unable to estimate the level of emission reduction efforts during this period. Finally, a generalized linear regression model (GLM) based only on meteorological parameters was built to predict air pollutant concentrations, which could explain more than 70 % of the variation in air pollutant concentration levels, after incorporating the nonlinear relationships between certain meteorological parameters and the concentrations of air pollutants. Evaluation of the GLM performance revealed that the GLM, even based only on meteorological parameters, could

be satisfactory to estimate the contribution of meteorological conditions in reducing air pollution and, hence, the contribution of control strategies in reducing air pollution. Using the GLM, we found that the meteorological conditions and pollution control strategies contributed 30 and 28 % to the reduction of the $\text{PM}_{2.5}$ concentration during APEC and 38 and 25 % during the Victory Parade, respectively, based on the assumption that the concentrations of air pollutants are only determined by meteorological conditions and emission intensities. We also estimated the contribution of meteorological conditions and control strategies in reducing the concentrations of gaseous pollutants and $\text{PM}_{2.5}$ components with the GLMs, revealing the effective control of anthropogenic emissions.

1 Introduction

Air pollution poses serious health risks to human populations and is one of the most important global environmental problems. To control air pollution in China, the State Council of China (2013) has released the Action Plan for Air Pollution Prevention and Control, which sets pollution control targets for different regions: e.g., atmospheric particulate matter of aerodynamic diameter $\leq 2.5 \mu\text{m}$ ($\text{PM}_{2.5}$) concentrations in 2017 should fall in Beijing–Tianjin–Hebei by 25 %, in the Yangtze River Delta by 20 %, and in the Pearl River Delta by 15 % compared with the levels of 2012. To meet these targets, comprehensive pollution control strategies have

been implemented at the national, provincial, and city levels. However, it is not clear how effective these strategies are in reducing air pollution. One of the challenges in evaluating the effectiveness of these strategies is that the long-term strategies cannot improve air quality in the short term. The efforts made to ensure satisfactory air quality for special events in the short term, such as the Beijing 2008 Olympics, provide a unique opportunity to evaluate the effectiveness of pollution control strategies (Kelly and Zhu, 2016). During the Beijing Olympics comprehensive pollution control strategies were implemented intensively over a short period of time. Based on the successful experience during this event, the Chinese government implemented similar air pollution control measures for the 41st Shanghai World Expo in 2010 (Huang et al., 2012; SEPB, 2010), the 16th Guangzhou Asian Games and Asian Para Games in 2010 (GEPB, 2009; Liu et al., 2013), and the Chengdu Fortune Forum 2013 (CEPB, 2013). To ensure satisfactory air quality in Beijing during the two most recent events, the Asia-Pacific Economic Cooperation Forum (APEC) 2014 and the 2015 China Victory Day Parade (Victory Parade 2015), the Chinese central government and the local government of Beijing, together with its surrounding provinces, implemented comprehensive air pollution control strategies. These two events provide a good opportunity to evaluate the effectiveness of air pollution control strategies.

One challenge when evaluating the effectiveness of air pollution control strategies over a short period of time is separating out the contribution of meteorological conditions to the reduction in air pollution levels.

Most previous studies have only provided a descriptive analysis of the changing concentrations of air pollutants during these events. Wen et al. (2016) reported that the average $\text{PM}_{2.5}$ concentration during APEC decreased by 54, 26, and 39 % compared with the levels before APEC in Beijing, Shijiazhuang, and Tangshan, respectively. Han et al. (2015) observed that the extinction coefficient and absorbance coefficient decreased significantly during APEC compared with the values before APEC.

An increasing number of studies have recognized the importance of meteorological conditions in determining air pollution in Beijing and North China Plain (Calkins et al., 2016; Zhang et al., 2012). A northerly wind is considered to be favorable for pollutant diffusion, while a southerly wind is considered to be favorable for the transport of pollutants to Beijing (Zhang et al., 2014). When assessing the effectiveness of air pollution control strategies, a few studies have distinguished between the contribution of meteorological conditions and pollution control strategies in reducing air pollution by comparing air pollutant concentrations under similar meteorological conditions (Wang et al., 2015; Zhang et al., 2009). However, in these studies, days with stable meteorological conditions were determined subjectively, which may introduce uncertainties and inconsistencies when estimating changes in air pollutant concentrations.

Statistical models have been developed to establish the relationship between air pollutant concentrations and meteorological parameters. Table 1 summarizes these models, with their respective R^2 values. Multiple linear regression models have been widely applied to demonstrate the quantitative relationship between air pollutant concentrations and meteorological parameters by assuming a linear relationship. However, these relationships are often nonlinear (Liu et al., 2007, 2012). Most of the models with good explanation ($R^2 > 0.6$) have actually adopted visibility, aerosol optical depth (AOD), and air quality index (AQI) as independent variables to improve the performance of the regression models (Liu et al., 2007; Sotoudeheian and Arhami, 2014; Tian and Chen, 2010; You et al., 2015). This could cause problems in the prediction of air pollutant concentrations during intensive emission control periods because visibility, AOD, and AQI are also dependent on air pollution levels; hence, the statistical models may not function when air pollutant levels are drastically reduced over a short period. A statistical model based solely on meteorological parameters to predict air pollutant concentrations is therefore required.

In this study, we used the air pollution control periods during APEC 2014 and Victory Parade 2015 to estimate the role of meteorological conditions and pollution control strategies in reducing air pollution in the megacity of Beijing. We first measured the changes in air pollutant concentrations, including $\text{PM}_{2.5}$, gaseous pollutants, and the components of $\text{PM}_{2.5}$. We then estimated the role of meteorological conditions and pollution control strategies in reducing air pollution by comparing the pollutant concentrations during days with stable meteorological conditions. Finally, we developed a statistical model based only on meteorological parameters to evaluate the role of meteorological conditions and pollution control strategies in reducing the levels of air pollution in Beijing.

2 Measurements and methods

2.1 Measurements

2.1.1 Measurements of air pollutants

Gaseous pollutants (SO_2 , NO , NO_x , and O_3) were measured online, and $\text{PM}_{2.5}$ samples were collected on filters at an urban monitoring station in the campus of Peking University (39.99° N, 116.33° E) northwest of Beijing (Huang et al., 2010). The station is located on the roof of a six-floor building, about 20 m above the ground and about 550 m north of the Fourth Ring Road of Beijing.

A $\text{PM}_{2.5}$ four-channel sampler (TH-16A, Wuhan Tianhong Instruments Co., Ltd., Hubei, China) was used to collect $\text{PM}_{2.5}$ samples. The sampling duration was 23.5 h (from 09:30 to 09:00 LT the next day). Both 47 mm quartz filters (QM/A, Whatman, Maidstone, England) and Teflon filters (PTFE, Whatman) were used. The flow rate was calibrated to

Table 1. Summary of statistical models applied to predict air pollutant concentrations with meteorological parameters.

Dependent variables	Independent variables	R^2	Methods ¹	Applications
PM _{2.5}	meteorological parameters (T , RH, PBL, WS, cloud fraction), AOT	0.47	MLR	Gupta and Christopher (2009)
PM ₁₀	meteorological parameters (T , WD, RH, PBL, WS), AOD	0.21, 0.30 (MODIS, MISR ²)	MLR	Sotoudeheian and Arhami (2014)
PM ₁₀	meteorological parameters (RH, WS, T), AOD	0.49–0.88 (spatial–temporal variability)	MLR	Chitranshi et al. (2015)
PM _{2.5}	meteorological parameters (T , RH, PREC), AOT	0.60, 0.58 (MOD, MYD ³)	MLR	Nguyen et al. (2015)
ln(PM _{2.5}), ln(PM _{2.5–10})	meteorological parameters (ln(PREC), ln(RH), ln(WS), ln(SUN), ln(T)), atmospheric turbulence parameters (ln(u/z), ln(θ/z))	0.60–0.74	GLM	Hien et al. (2002)
ln(PM _{2.5})	meteorological parameters (T , WD, ln(WS), ln(PBL)), ln(AOT), categorical parameters	0.51, 0.62 (MODIS, MISR)	GLM	Liu et al. (2007)
log(PM _{2.5}), log(BC)	meteorological parameters (T , wind index), traffic-related parameters	0.62, 0.42 (PM _{2.5} , BC)	GLM	Richmond-Bryant et al. (2009)
ln(PM _{2.5})	meteorological parameters (ln(PBL), GEO-4 RH, ln(surface RH), T), ln(AOD)	0.65	GLM	Tian and Chen (2010)
ln(PM ₁₀)	meteorological parameters (T , WD, RH, ln(PBL), ln(WS)), ln(AOD)	0.18, 0.38 (MODIS, MISR)	GLM	Sotoudeheian and Arhami (2014)
ln(PM _{2.5})	meteorological parameters (ln(PBL), RH, Vis, ln(T), ln(WS)), ln(AOD)	0.67, 0.72 (MODIS, MISR)	GLM	You et al. (2015)
ln(PM _{2.5})	meteorological parameters (WS, WD, T , RH, pressure), optical properties (absorption, scattering, attenuation coefficient)	0.54, 0.31, 0.32, 0.88 (winter, pre-monsoon, monsoon, post-monsoon)	GLM	Raman and Kumar (2016)
PM ₁₀ , PM _{2.5}	smooth non-parametric functions of spatial, temporal variates	0.58	GAM	Barmpadimos et al. (2012)
PM _{2.5} , PM ₁₀ , PM _{2.5–10}	smooth non-parametric functions of spatial, temporal variates	0.77, 0.58, 0.46– 0.52 (PM _{2.5} , PM ₁₀ , PM _{2.5–10})	GAM	Yanosky et al. (2014)
PM ₁₀	meteorological parameters (WS, T_{\min} , T_{\max}), previous day PM ₁₀	0.78	ANN	Diaz-Robles et al. (2008)
PM _{2.5}	meteorological parameters (WS, RH, PBL, WS*PBL), AOD, spatial explanatory variables	0.89	LUR	Chudnovsky et al. (2014)
PM ₁₀ , NO ₂	meteorological parameters (T , RH, WS, air pressure, cloud cover, percentage of haze, mist, rain, sun), spatial explanatory variables	0.45, 0.43 (PM ₁₀ , NO ₂)	LUR	Liu et al. (2015)

¹ MLR: multiple linear regression model; GLM: generalized linear regression model; GAM: generalized additive model; ANN: artificial neural networks; LUR: land use regression model.

² MODIS: Moderate Resolution Imaging Spectroradiometer; MISR: Multi-Angle Imaging Spectroradiometer.

³ MOD, MYD: MODIS Terra (AM overpass) and Aqua (PM overpass).

16.7 L min⁻¹ each week and a blank PM_{2.5} sample was collected once a month. The quartz filters were baked at 550 °C

for 5.5 h before use. Immediately after collection, the filter samples were stored at -25 °C until analysis.

Sulfur dioxide (SO₂) was measured with an SO₂ analyzer (43i TL, Thermo Fisher Scientific, Waltham, MA, USA), with a precision of 0.05 ppb. Nitric oxide (NO) and nitrogen oxides (NO_x) were measured with a NO–NO_x analyzer (42i TL, Thermo Fisher Scientific), with precisions of 0.05 ppb for NO and 0.17 ppb for NO₂. Ozone (O₃) was measured with an O₃ analyzer (49i, Thermo Fisher Scientific), with a precision of 1.0 ppb. The SO₂ and NO–NO_x analyzers both had a detection limit of 0.05 ppb, and the O₃ analyzer had a detection limit of 0.50 ppb. All of the gaseous pollutant analyzers had a time resolution of 1 min and were maintained and calibrated weekly following the manufacturer's protocols.

2.1.2 Meteorological data

Meteorological data were obtained from the National Climate Data Center (www.ncdc.noaa.gov) dataset. The meteorological parameters were monitored at a station located in the Beijing Capital International Airport, and consisted of temperature (*T*), relative humidity (RH), wind direction (WD), wind speed (WS), sea level pressure (SLP), and precipitation (PREC). The planetary boundary layer (PBL) height was computed from the simulation results of the National Center for Environmental Prediction (NCEP) Global Data Assimilation System (GDAS) model (<https://ready.arl.noaa.gov/archives.php>).

2.1.3 Analysis of the PM_{2.5} filter samples

To obtain daily average PM_{2.5} mass concentrations, Teflon filters were weighed before and after sampling using an electronic balance, with a detection limit of 10 μg (AX105DR) in a super-clean lab (*T*: 20 ± 1 °C; RH: 40 ± 3 %). A portion of each Teflon filter was extracted with ultrapure water for the measurement of water-soluble ions (Na⁺, NH₄⁺, K⁺, Mg²⁺, Ca²⁺, SO₄²⁻, NO₃⁻, and Cl⁻), with an ion chromatograph (IC-2000 and 2500, Dionex, Sunnyvale, CA, USA). The detection limits of Na⁺, NH₄⁺, K⁺, Mg²⁺, Ca²⁺, SO₄²⁻, NO₃⁻, and Cl⁻ were 0.03, 0.06, 0.10, 0.10, 0.05, 0.01, 0.01, and 0.03 mg L⁻¹, respectively. A portion of each Teflon filter was digested with a solution consisting of nitric acid (HNO₃), hydrochloric acid (HCl), and hydrofluoric acid (HF) for the measurement of trace elements (Na, Mg, Al, Ca, Mn, Fe, Co, Cu, Zn, Se, Mo, Cd, Ba, Tl, Pb, Th, and U), with inductively coupled plasma–mass spectrometry (ICP-MS, Thermo X series, Thermo Fisher Scientific). The recoveries for all measured elements fell within ±20 % of the certified values. A semi-continuous organic carbon–elemental carbon (OC/EC) analyzer (Model 4, Sunset Laboratory, Tigard, OR, USA) was used to analyze organic and elemental carbon from a round punch (diameter: 17 mm) from each quartz filter sample. The T protocol of the National Institute for Occupational Safety and Health (NIOSH) thermal–optical method was applied (see details in Table S1 in the Supplement).

All analytical instruments were calibrated before each series of measurements. The *R*² values of the calibration curves for ions, elements, and sucrose concentrations were higher than 0.999.

2.2 Research periods definition and control strategies

In our study, the APEC 2014 campaign consisted of three distinct periods: before APEC (18 October to 2 November 2014), during APEC (3 to 12 November 2014), and after APEC (13 to 22 November 2014). The Victory Parade 2015 campaign was also divided into three distinct periods: before the parade (1 to 19 August 2015), during the parade (20 August to 3 September 2015), and after the parade (4 to 23 September 2015). A total of 225 PM_{2.5} filter samples were collected from 1 October to 31 December 2014 and from 1 August to 31 December 2015. A sufficient number of sampling days is used to establish the relationship between air pollutant concentrations and meteorological parameters. Twenty days of PM_{2.5} samples were missed due to rain or sampler failures.

Table 2 shows the control periods and control strategies of APEC and the Victory Parade, including the control of emissions from traffic, industry, and coal combustion, as well as dust pollution.

2.3 Methods for the meteorological conditions separation

2.3.1 Identify stable meteorological periods

Stable conditions can be defined based on the relationship between air pollution levels and both WS and PBL height. Figure 5 shows scatter plots between PM_{2.5} concentrations and WS and PBL heights. The relationship can be fitted with a power function. A stable condition could be defined by identifying the turning points when the slopes changed from large to relatively small values, and stable conditions could be defined when WSs and PBL heights were lower than the values of the turning points.

The slopes of the power function were monotone, varying with no inflection point. Thus, we used piecewise functions to identify the turning points. As Fig. 5 shows, the intersections of two fitting lines represented the turning points of the meteorological influence on PM_{2.5}; thus, we defined days with stable meteorological conditions to be those with a daily average WS less than 2.50 ms⁻¹ and a daily average PBL height lower than 290 m. We could then compare the corresponding pollutant concentrations between days with stable meteorological conditions.

2.3.2 Generalized linear regression model (GLM)

A GLM was used to establish the relationship between air pollutant concentrations and meteorological parameters. The objective dependent variables included concentrations

Table 2. Air pollution control strategies during APEC 2014 and Victory Parade 2015.

Periods	Control measures	Detail of measures
APEC 2014 (3 to 12 Nov 2014) and Victory Parade 2015 (20 Aug to 3 Sep 2015)	Traffic control	The odd/even plate number rule for traffic control in Beijing, Tianjin, Hebei, and Shandong; 70 % (APEC 2014)/80 % (Victory Parade 2015) of official vehicle and “yellow label vehicles” were banned from Beijing’s roads; trucks were limited to run inside the Sixth Ring Road between 06:00 to 24:00.
	Industrial emission control	More than 10 000 factories production limited or halted in Beijing and Hebei, Tianjin, Shandong, Shanxi, and Inner Mongolia, which surround Beijing.
	Dust pollution control	Dust emission factories and outdoor constructions shut down or limited in Beijing and nearby area; enhancing road cleaning and spray and dust collection in Beijing.
	Coal-fired control	State-owned enterprise productions enhancing limited and 40 % coal-fired boilers shut down in Beijing; more special pollutant emission factory limited around Beijing.

of PM_{2.5}, individual PM_{2.5} components, and gaseous pollutants.

To match the 23.5 h (09:30–09:00 LT the next day) sampling time of the PM_{2.5} filter samples, meteorological parameters were averaged over the same time span (Table 3) and used in the GLM alongside other parameters, e.g., the daily maximum of certain meteorological parameters. The meteorological parameters used in the GLM were T, RH, WD, WS, PBL height, SLP, and PREC. WDs were grouped into three categories, with relevant values and assigned to each category: north (NW, W, and NE) as 1, south (SW, SE, and E) as 2, and “calm and variable” as 3. A calm wind was defined as when the WS was less than 0.5 m s⁻¹. According to the Jet-Stream Glossary of NOAA (http://www.srh.weather.gov/srh/jetstream/append/glossary_v.html), a variable WD was defined as a condition when (1) the WD fluctuated by 60° or more during a 2 min evaluation period, with a WS greater than 6 knots (11 km h⁻¹) or (2) the WD was variable and the WS was less than 6 knots (11 km h⁻¹).

A preliminary analysis showed that the concentrations of air pollutants and meteorological parameters fitted best with an exponential function or power function (Fig. S2); therefore, these functions were natural log transformed and introduced into the GLM.

We applied the stepwise method to evaluate the level of multicollinearity between the independent variables based on relevant judgement indexes, such as the variance inflation factor (VIF) or tolerance. Based on the assumption that the regression residuals followed a normal distribution and homoscedasticity, which is discussed in a later section, we developed the following model to calculate the concentrations of air pollutants and chemical components of PM_{2.5} based on

meteorological parameters:

$$\ln C_{ij} = \beta_0 + \sum_{k=1}^m \beta_{1k} x_k + \sum_{k=1}^n \beta_{2k} \ln x_k + \sum_{k=1}^{m'} \beta_{3k} x_k(\text{lag}) + \sum_{k=1}^{n'} \beta_{4k} \ln x_k(\text{lag}), \quad (1)$$

where C_{ij} is the concentration of the j th air pollutant averaged over the i th day, x_k is the k th meteorological parameter, β_k is the regression coefficient of the k th meteorological parameter, and β_0 is the intercept. For meteorological parameters containing both positive and negative values (i.e., T), only the exponential form was applied. m , n , m' , and n' are the number of different forms of meteorological parameters that were eventually included in the model and were determined based on the stepwise entering method of the regression model. The suffix of (lag) refers to the meteorological parameters of the previous day. The main assumption for Eq. (1) was that the concentrations of air pollutants were only a function of the meteorological parameters and that the emission intensities were constant. Hence, we only used the data before and after APEC 2014 and Victory Parade 2015 control periods in Eq. (1), excluding the data collected during each period and during the heating season, e.g., after 15 November 2014.

Compared with the models used in previous studies (Table 1), our statistical model had the following advantages: (1) all of the independent variables were meteorological parameters; (2) we considered the nonlinear relationships between air pollutant concentrations and meteorological parameters; and (3) in addition to predicting PM_{2.5} mass concentrations, our model could also predict concentrations of gaseous pollutants and individual PM_{2.5} components by corresponding models for different pollutants.

Table 3. Meteorological parameters used in the GLM in this study. The calculation of each meteorological parameter is based on the sample duration of 23.5 h (09:30–09:00 LT the next day).

Parameters	Abbreviations	Description
Wind direction value ^a	WD	The average of wind direction values
	WD _{sum}	The sum of wind direction values
	WD _{mode}	The mode of wind direction values
Wind speed (m s ⁻¹)	WS	The average of wind speed
	WS _{mode}	The mode of wind speed
	WS _{max}	The maximum of wind speed
Temperature (°C)	<i>T</i>	The average of temperature
	<i>T</i> _{max}	The maximum of temperature
	<i>T</i> _{min}	The minimum of temperature
	<i>T</i>	The difference of temperature
Sea level pressure (hPa)	SLP	The average of sea level pressure
	SLP _{max}	The maximum of sea level pressure
	SLP _{min}	The minimum of sea level pressure
Relative humidity (%)	RH	The average of relative humidity
	RH _{max}	The maximum of relative humidity
Precipitation (mm)	PREC	The accumulation of precipitation
Wind index	WD/WS	The average of wind direction value divided by wind speed
	WD/WS _{sum}	The sum of wind direction value divided by wind speed
Planetary boundary layer height (m)	PBL	The average of 3 h planetary boundary layer height
	PBL _{min}	The minimum of 3 h planetary boundary layer height
	PBL _{max}	The maximum of 3 h planetary boundary layer height

^a Since the degree data of wind direction cannot be applied directly, the values of wind directions are donated such that value = 1, 2, 3 for north, south, and “calm and variable”, respectively.

3 Results and discussion

3.1 Changes of air pollutant concentrations during the APEC 2014 and Victory Parade 2015 campaigns

Figure 1 shows the time series of PM_{2.5} and the concentrations of its components, as well as the meteorological parameters during the APEC 2014 and Victory Parade 2015 campaigns.

There were two pollution episodes during APEC, 4 November and 7–10 November 2014, which corresponded to two relatively stable periods with low WS, mainly from the south. The *T* declined gradually from 12.2 °C before APEC to 4.9 °C after APEC, and the RH was above 60 % during the two pollution episodes. During the parade, the PM_{2.5} concentrations were low, with the prevailing WD from the north and low WS. The *T* was mostly higher than 20 °C, which differed from that during the APEC campaign when it was lower than 20 °C.

Table 4 lists the mean concentrations and SDs of PM_{2.5}, gaseous pollutants, and PM_{2.5} components during the APEC and Victory Parade campaigns. The mean concentration of PM_{2.5} during APEC was 48 ± 35 μg m⁻³, 58 % lower than before APEC (113 ± 62 μg m⁻³) and 51 % lower than after APEC (97 ± 84 μg m⁻³). The mean concentration of PM_{2.5} during the parade was 15 ± 6 μg m⁻³, 63 % lower than before

the parade (41 ± 14 μg m⁻³) and 62 % lower than after the parade (39 ± 28 μg m⁻³).

Figure 2 shows the proportion of the measured PM_{2.5} components, including OC; EC; the sum of the sulfate, nitrate, and ammonia (SNA); and chloride ion (Cl⁻) and trace elements, which together accounted for 70–80 % of the total PM_{2.5} mass concentration. The proportions of OC (23.5 %) and EC (3.5 %) in PM_{2.5} were highest during APEC. The proportion of SNA in PM_{2.5} during APEC (40.6 %) was lower than before APEC (50.7 %) and higher than after APEC (37.2 %). The proportions of Cl⁻ (4.3 %) and elements (6.8 %) in PM_{2.5} during APEC were higher than before APEC and lower than after APEC. For the parade campaign, the proportions of OC (26.6 %) and elements (6.6 %) in PM_{2.5} were highest during the parade. The proportions of EC (4.9 %) and Cl⁻ (1.1 %) in PM_{2.5} during the parade were higher than before the parade and lower than after the parade. The proportion of SNA in PM_{2.5} was lowest during the parade (37.3 %). Similarly, during the pollution control periods of APEC and the parade, the proportions of OC and elements in PM_{2.5} tended to increase and the proportion of SNA in PM_{2.5} tended to decrease.

EC is usually considered to be a marker of anthropogenic primary sources, while the sources of OC include both primary and secondary organic aerosols. The correlation between OC and EC can reflect the origin of carbonaceous fractions (Chow et al., 1996). Figure 3 shows the correlation be-

Table 4. Statistical summary showing the mean concentrations and SDs of PM_{2.5}, gaseous pollutants, and PM_{2.5} components. BAPEC and BParade: before APEC and before Victory Parade; AAPEC and AParade: after APEC and after Victory Parade.

Pollutants	Units	BAPEC	APEC	AAPEC	BParade	Parade	AParade
PM _{2.5}	μg m ⁻³	113 ± 62	48 ± 35	97 ± 84	41 ± 14	15 ± 6	39 ± 28
OC		15.3 ± 8.7	11.2 ± 7.2	21.3 ± 15.5	7.4 ± 1.9	4.0 ± 1.0	6.3 ± 3.1
EC		2.7 ± 1.4	1.7 ± 1.0	3.5 ± 1.8	1.6 ± 0.3	0.8 ± 0.1	2.0 ± 1.0
SO ₄ ²⁻		12.6 ± 9.1	3.9 ± 3.0	9.6 ± 12.4	10.6 ± 6.2	2.6 ± 1.3	7.9 ± 7.3
NO ₃ ⁻		29.4 ± 21.4	10.6 ± 11.0	16.3 ± 19.4	5.0 ± 3.9	1.5 ± 1.5	6.4 ± 6.2
NH ₄ ⁺		15.0 ± 10.6	4.8 ± 4.2	10.3 ± 11.9	5.2 ± 2.6	1.5 ± 1.0	5.4 ± 5.4
Cl ⁻		3.19 ± 1.61	2.06 ± 2.11	6.59 ± 6.67	0.20 ± 0.16	0.16 ± 0.12	0.53 ± 0.24
Na ⁺		0.50 ± 0.26	0.26 ± 0.15	0.57 ± 0.46	0.16 ± 0.09	0.10 ± 0.05	0.16 ± 0.08
K ⁺		1.20 ± 0.63	0.65 ± 0.51	1.52 ± 1.43	0.30 ± 0.13	0.18 ± 0.08	0.38 ± 0.20
Mg ²⁺		0.07 ± 0.03	0.09 ± 0.02	0.13 ± 0.07	0.01 ± 0.01	0.01 ± 0.00	0.02 ± 0.01
Ca ²⁺		0.52 ± 0.34	0.28 ± 0.19	0.53 ± 0.40	0.14 ± 0.07	0.10 ± 0.04	0.17 ± 0.05
SO ₂		11.3 ± 5.0	9.5 ± 6.8	34.8 ± 15.3	2.7 ± 1.6	1.6 ± 1.4	5.9 ± 5.2
NO		54.2 ± 30.5	21.9 ± 13.8	112.3 ± 63.2	3.2 ± 2.1	1.2 ± 0.9	9.3 ± 7.5
NO _x		151 ± 62	81 ± 46	220 ± 107	57 ± 11	26 ± 13	63 ± 24
O ₃		23 ± 16	38 ± 19	17 ± 14	116 ± 33	79 ± 22	74 ± 27
Ca	ng m ⁻³	582 ± 431	591 ± 335	1536 ± 579	202 ± 64	108 ± 36	188 ± 130
Co		0.48 ± 0.21	0.34 ± 0.18	0.90 ± 0.52	0.21 ± 0.08	0.05 ± 0.02	0.16 ± 0.10
Ni		3.20 ± 1.56	5.07 ± 7.42	5.17 ± 2.50	1.75 ± 1.16	0.63 ± 0.72	1.16 ± 0.67
Cu		35.7 ± 16.2	19.1 ± 12.6	43.3 ± 31.2	12.4 ± 5.1	3.7 ± 1.3	9.6 ± 6.5
Zn		320 ± 146	128 ± 120	315 ± 310	97 ± 46	20 ± 9	71 ± 54
Se		6.45 ± 3.46	3.76 ± 3.84	5.22 ± 6.56	7.06 ± 3.41	3.19 ± 2.76	3.17 ± 2.76
Mo		2.20 ± 1.12	1.63 ± 1.14	2.85 ± 2.67	0.62 ± 0.41	0.16 ± 0.14	0.53 ± 0.46
Cd		3.86 ± 2.53	1.41 ± 1.25	3.11 ± 2.52	2.35 ± 5.72	0.22 ± 0.17	0.71 ± 0.74
Tl		1.87 ± 0.90	0.87 ± 1.01	2.03 ± 1.96	0.50 ± 0.31	0.05 ± 0.06	0.33 ± 0.39
Pb		121 ± 59	55 ± 52	104 ± 81	36 ± 19	9 ± 6	29 ± 26
Th		0.09 ± 0.05	0.06 ± 0.03	0.09 ± 0.06	0.02 ± 0.01	0.01 ± 0.01	0.01 ± 0.01
U		0.06 ± 0.02	0.05 ± 0.03	0.09 ± 0.06	0.02 ± 0.01	0.00 ± 0.00	0.01 ± 0.02
Na		529 ± 261	355 ± 209	907 ± 632	182 ± 71	96 ± 39	181 ± 96
Mg		153 ± 94	105 ± 47	236 ± 143	43 ± 13	15 ± 8	24 ± 15
Al		516 ± 324	338 ± 154	588 ± 406	141 ± 82	130 ± 60	136 ± 93
Mn		55.5 ± 23.3	34.5 ± 24.1	61.6 ± 52.4	17.3 ± 6.4	3.6 ± 1.8	14.8 ± 9.2
Fe		755 ± 314	573 ± 336	883 ± 538	269 ± 71	98 ± 28	234 ± 139
Ba		16.3 ± 8.0	11.0 ± 8.4	13.8 ± 8.1	4.7 ± 1.6	1.9 ± 0.6	4.1 ± 2.3

Table 5. The cross-validation (CV) performance of the PM_{2.5} GLM.

Periods	Adjusted R^2	Observed mean values (μg m ⁻³)	Predicted mean values (μg m ⁻³)	Daily RMSE (μg m ⁻³)	Total RMSE (μg m ⁻³)	Relative errors ^a	Mean relative error	RMSE of relative error
CV1	0.748	94	82	53	33	15 %	-5 %	14.6 %
CV2	0.798	59	57	20		4 %		
CV3	0.783	44	52	19		-15 %		
CV4	0.710	54	65	27		-17 %		
CV5	0.807	41	47	30		-13 %		

^a Relative error = (predicted mean value - observed mean value) / predicted mean value × 100 %.

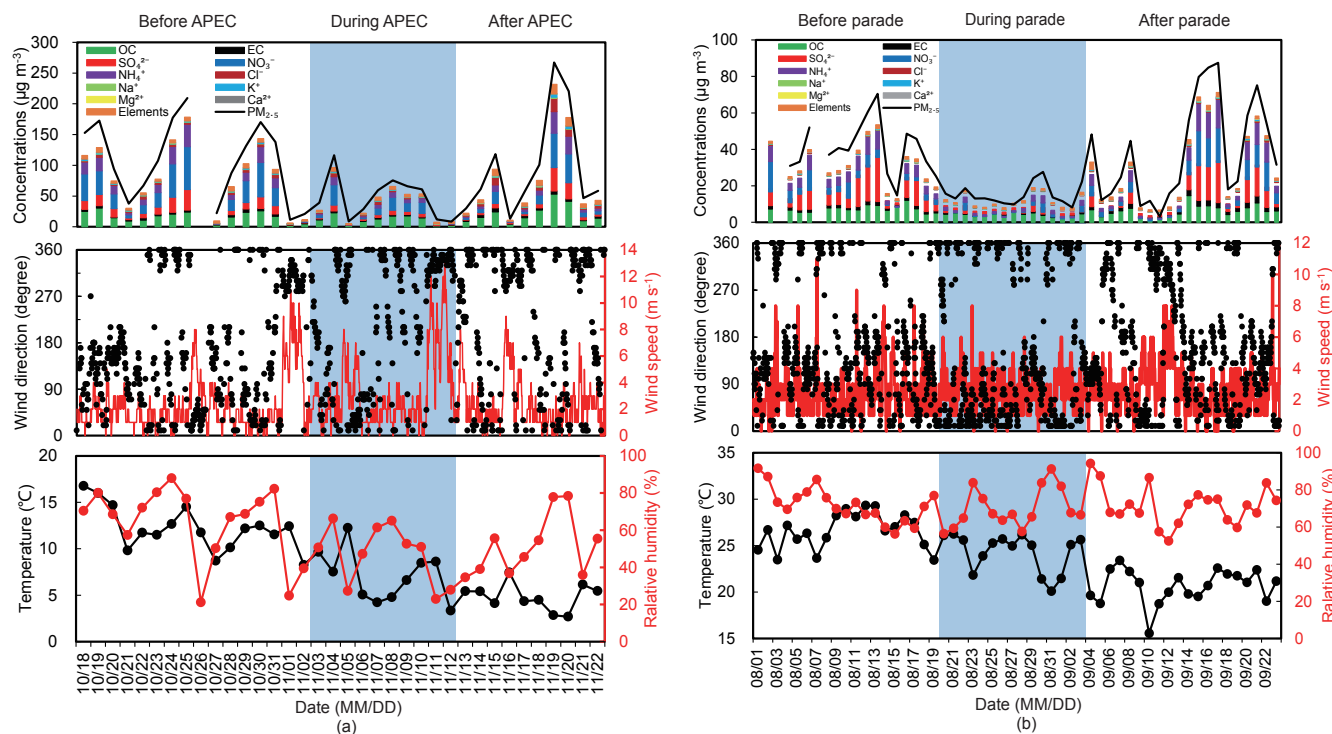


Figure 1. Time series of atmospheric particulate matter of aerodynamic diameter $\leq 2.5 \mu\text{m}$ ($\text{PM}_{2.5}$) and the concentrations of its components, wind direction (WD), wind speed (WS), temperature (T), and relative humidity (RH) before, during, and after (a) APEC 2014 and (b) Victory Parade 2015. The blue-shaded areas highlight the pollution control periods of APEC 2014 (3 November to 12 November 2014) and Victory Parade 2015 (20 August to 3 September 2015).

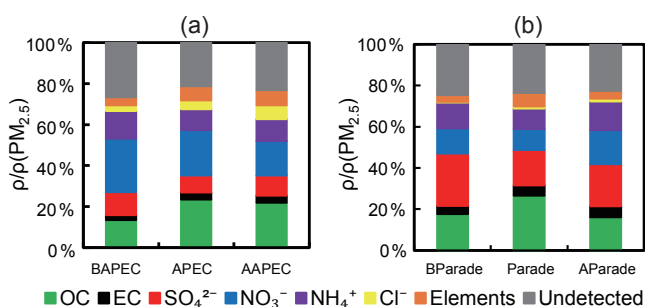


Figure 2. Proportions of the measured components in $\text{PM}_{2.5}$ during (a) APEC 2014 and (b) Victory Parade 2015 campaigns, including organic carbon (OC), elemental carbon (EC), SO_4^{2-} , NO_3^- , NH_4^+ , Cl^- , and elements. BAPEC and BParade: before APEC and before Victory Parade; AAPEC and AParade: after APEC and after Victory Parade.

tween EC and OC concentrations during the APEC and Victory Parade campaigns. During the APEC and Victory Parade campaigns, the correlation coefficient during both control periods ($R^2 = 0.9032$) was larger than that during non-control periods ($R^2 = 0.6468$), indicating that OC and EC were mainly derived from the same sources during both pollution control periods and were from different sources during the non-control periods. Li et al. (2017) reported that the resi-

dential burning of coal and open and domestic combustion of wood and crop residuals could contribute to more than 50 % of total organic aerosol of the North China Plain during winter. During the control periods, it might be difficult to fully control the emission of residential burning. The slope of the OC/EC correlation during the pollution control period was 6.86, which was higher than that during the non-control period (3.97). This could be due to high levels of secondary OC (SOC) formation during the control periods and/or the higher contribution from residential solid fuel (coal and biomass) burning (Liu et al., 2016).

Figure 4 shows the proportion of SNA in $\text{PM}_{2.5}$ (ρ ($\text{SNA}/\text{PM}_{2.5}$)), the sulfur (S) oxidation ratio ($\text{SOR} = [\text{SO}_4^{2-}] / ([\text{SO}_2] + [\text{SO}_4^{2-}])$), and nitrogen oxidation ratio ($\text{NOR} = [\text{NO}_3^-] / ([\text{NO}_x] + [\text{NO}_3^-])$), along with $\text{PM}_{2.5}$ concentrations during the APEC (a) and Victory Parade (b) campaigns. During APEC, the average ρ ($\text{SNA}/\text{PM}_{2.5}$) was 27 %, which was significantly lower than before APEC (42 %). During the parade, the average ρ ($\text{SNA}/\text{PM}_{2.5}$) was 35 %, which was also significantly lower than before the parade (47 %).

During the APEC campaign, the average SO_2 concentration was $11.3 \mu\text{g m}^{-3}$ before APEC, $9.5 \mu\text{g m}^{-3}$ during APEC, and $34.8 \mu\text{g m}^{-3}$ after APEC. The average NO_x concentration was $151 \mu\text{g m}^{-3}$ before APEC, $81 \mu\text{g m}^{-3}$ during

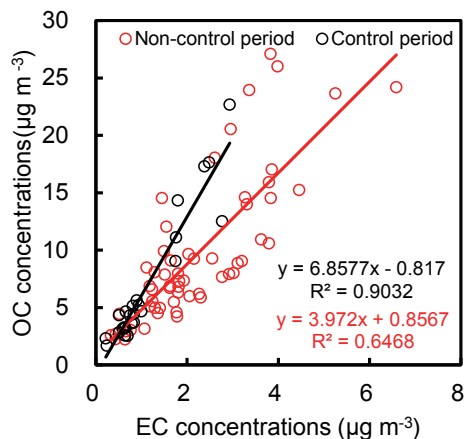


Figure 3. Scatter plot and correlations between organic carbon (OC: y axis) and elemental carbon (EC: x axis) concentrations of $\text{PM}_{2.5}$ during the APEC 2014 and Victory Parade 2015 campaigns. The red symbols denote the non-control period and the black symbols denote the pollution control period. The linear regression equations and R^2 values are given for these two campaigns.

APEC, and $220 \mu\text{g m}^{-3}$ after APEC. During the parade campaign, the average SO_2 concentration during the parade was $1.6 \mu\text{g m}^{-3}$, lower than both before the parade ($2.7 \mu\text{g m}^{-3}$) and after the parade ($5.9 \mu\text{g m}^{-3}$). The average NO_x concentration was also lower during the parade ($26 \mu\text{g m}^{-3}$) than before the parade ($57 \mu\text{g m}^{-3}$) and after the parade ($63 \mu\text{g m}^{-3}$).

During the APEC campaign, both the SOR and NOR declined gradually. The average SOR was 42, 27, and 17 % before, during, and after APEC, respectively. The average NOR was 13, 8, and 5 % before, during, and after APEC, respectively. SOR and NOR exhibited different patterns during the parade campaign. The average SOR was 75, 64, and 55 % before, during, and after the parade, respectively. The average NOR was 8, 5, and 8 % before, during, and after the parade, respectively. The SOR was higher during the parade campaign (64 %) than during the APEC campaign (30 %). For NOR, a higher average value was found during the APEC campaign (9 %) than during the parade campaign (7 %).

The APEC campaign occurred during autumn and early winter, while the parade campaign occurred during late summer and autumn. The active photochemical oxidation during the parade campaign resulted in high SO_2 -to-sulfate transformation rates, as indicated by the high SOR. In addition, the higher RH in summer favored the heterogeneous reaction of sulfate formation (Fig. 1). For NOR, the T was higher during the parade than during APEC, which favored the volatilization of nitric acid and ammonia from the particulate phase of nitrate.

These results indicate significant reductions of air pollution during the pollution control periods of APEC 2014 and Victory Parade 2015. However, it is necessary to evaluate if meteorological conditions contributed to this improvement.

3.2 Variation of air pollutant concentrations under similar meteorological conditions

Figure S3 shows the prevalence of WD during the APEC and Victory Parade campaigns. Figure S4 shows a time series of daily average $\text{PM}_{2.5}$ concentrations and PBL heights during the APEC and Victory Parade campaigns. Both WS and PBL height during the APEC and Victory Parade were favorable for pollutant diffusion. Therefore, it is necessary to consider meteorological conditions when assessing the impacts of pollution control. One way to do this is to compare air pollution concentrations during periods when meteorological conditions were the same, i.e., under stable conditions (Wang et al., 2015; Zhang et al., 2009).

The days with stable meteorological conditions were determined with the method introduced in Sect. 3.2.1. As a result, 8 days before APEC, 6 days during APEC, and 7 days after APEC were defined as having stable meteorological conditions (Table S5).

Figure 6 shows the percentage reductions calculated by comparing the decreased average concentrations for all days during APEC to the average concentrations before APEC in black bars and the percentage reductions based on the days with stable meteorological conditions in red bars. For the difference between the periods during APEC and before APEC, the percentage reduction on days with stable meteorological conditions was much lower than the reduction calculated when considering all days, except for Ca and NO. This indicates that the method applied to days with stable meteorological conditions excluded part of the meteorological influence on pollutant concentrations. The average $\text{PM}_{2.5}$ concentration was $70 \mu\text{g m}^{-3}$ during APEC, which represented a 45.7 % decrease compared with the concentration in the BAPEC period ($129 \mu\text{g m}^{-3}$) and a 44.4 % decrease compared with the concentration in the AAPEC period ($126 \mu\text{g m}^{-3}$) (Fig. S8). Changes of other pollutant concentrations on days with stable meteorological conditions during the APEC campaign are shown in Fig. S8.

The SDs were also calculated with an error transfer formula that is described in detail in the Supplement (S6). Figure 6 shows that the SDs of the percentage reduction based on days with stable meteorological conditions decreased significantly. For example, the SD of the percentage reduction in $\text{PM}_{2.5}$ based on the days with stable meteorological conditions decreased from 39 to 26 % compared with the same measurement when all days were considered. This indicates that by considering only days with stable meteorological conditions, the uncertainties associated with the percentage reduction figures were reduced and the reliability of the changes of air pollutants concentrations were improved. However, uncertainties remain within the percentage differences based on the days with stable meteorological conditions, although the size of these uncertainties was reduced. Table S7 lists the percentage differences among the mean $\text{PM}_{2.5}$ concentrations of four periods that were randomly se-

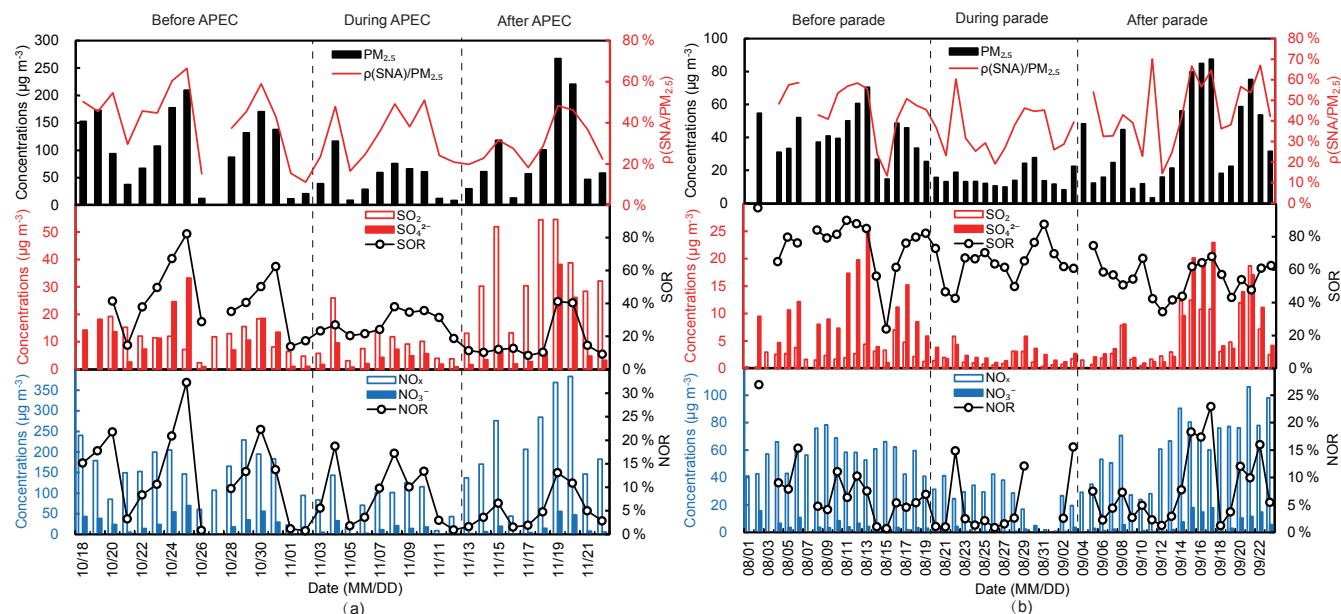


Figure 4. Upper panel: time series of the proportion of sulfate, nitrate, and ammonia (SNA) in $\text{PM}_{2.5}$ (ρ ; $\text{SNA}/\text{PM}_{2.5}$) and $\text{PM}_{2.5}$ mass concentrations (the black bar represents $\text{PM}_{2.5}$ concentration and the red line represents ρ ; $\text{SNA}/\text{PM}_{2.5}$). Middle panel: SO_2 , SO_4^{2-} , and SOR ($[\text{SO}_4^{2-}]/([\text{SO}_2]+[\text{SO}_4^{2-}])$). Lower panel: NO_x , NO_3^- , and NOR ($[\text{NO}_3^-]/([\text{NO}_x]+[\text{NO}_3^-])$). Data collected during the (a) APEC 2014 and (b) Victory Parade 2015 campaigns. The hollow bars represent gaseous pollutants (red for SO_2 , blue for NO_x), and solid bars represent secondary inorganic ions (red for sulfate, blue for nitrate).

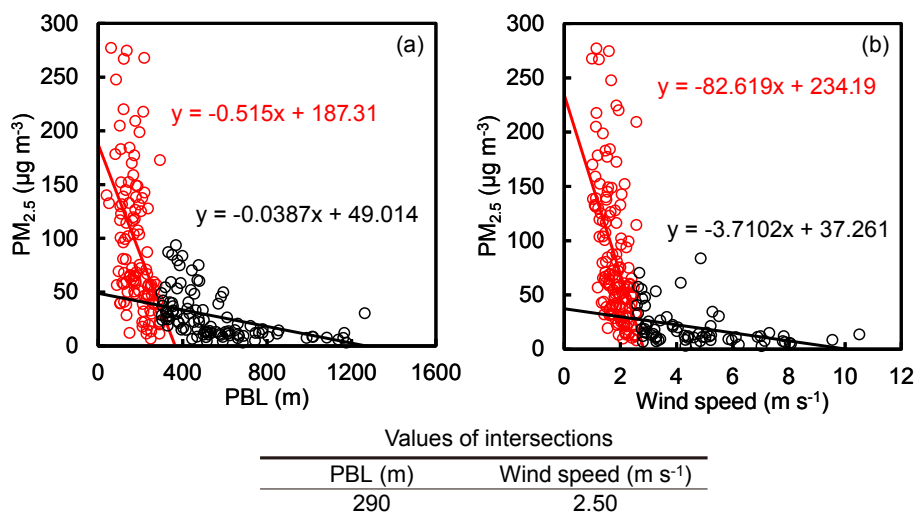


Figure 5. Scatter plot showing the correlation between daily $\text{PM}_{2.5}$ concentrations (y axis) and (a) daily PBL heights (x axis) and (b) daily wind speeds (x axis) during the sampling periods. The red and black scattered points represent different distribution areas. The piecewise function regression equations and the corresponding values of PBL height and wind speed according to the intersections are given.

lected from within the non-control days of the APEC and parade campaigns. This may be due to the limited sample size on days with stable meteorological conditions during the APEC campaign. It is therefore necessary to further quantify the meteorological influences.

3.3 Emission reductions during APEC and Victory Parade based on GLM predictions

The previous section showed that the number of days with stable meteorological conditions could be limited; it was therefore impossible to estimate quantitatively the contribution of meteorological conditions to the reduction of air pol-

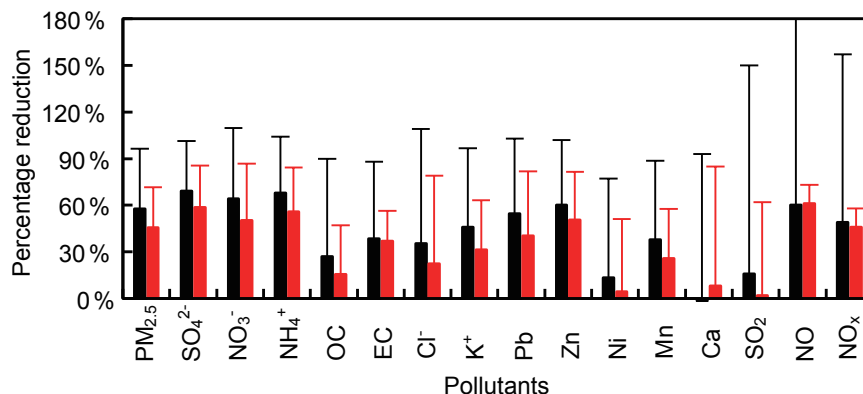


Figure 6. The percentage reductions of pollutant concentrations under similar meteorological conditions. The black bars represent the percentage reductions calculated by comparing the decreased average concentrations during APEC to the average concentrations before APEC. The red bars represent the percentage reductions calculated by comparing the decreased average concentrations during APEC to the average concentrations before APEC based only on the days with stable meteorological conditions. The whiskers represent the SDs of the percentage reductions.

lutant concentrations. We developed a GLM based only on meteorological parameters to meet this requirement.

3.3.1 Model performance and cross-validation (CV) test

Figure 7 shows the scatter plot and correlation between the GLM-predicted and observed concentrations of air pollutants transformed to a natural log. Figure 8 demonstrates the time series of the observed pollutant and GLM-predicted pollutant concentrations, which displayed a good correlation. The R^2 values of the linear regression equations ranged from 0.6638 to 0.8542, most of them are higher than 0.7 except for Zn and Mn, indicating that the GLM-predicted concentrations correlated well with the observed concentrations. Specifically, the R^2 value of the linear regression equation for $\text{PM}_{2.5}$ is as high as 0.8154.

Before applying the GLM to predict the air pollutant concentrations, the CV method was used to evaluate the performance of the $\text{PM}_{2.5}$ model, with the assumption that it was representative of all air pollutants. The data input to the $\text{PM}_{2.5}$ model was allocated randomly into five equal periods, namely CV1, CV2, CV3, CV4, and CV5. For each test, one period was removed from the input data and the remaining data were applied to establish the CV model, which was then used to predict the $\text{PM}_{2.5}$ concentrations for the removed period. After five rounds, all input data were included in the CV test. Figure 9 shows the time series of the observed and CV-predicted $\text{PM}_{2.5}$ concentrations, which demonstrates a good performance for the $\text{PM}_{2.5}$ GLM.

Table 5 shows the CV-predicted $\text{PM}_{2.5}$ concentrations. The adjusted R^2 values for the five CV periods ranged from 0.710 to 0.807, which was lower than the value (0.808) derived from the $\text{PM}_{2.5}$ model due to the lack of input data. The observed mean $\text{PM}_{2.5}$ concentrations were 94, 59, 44, 54, and

41 $\mu\text{g m}^{-3}$ for the five CV periods, respectively. The corresponding CV-predicted mean $\text{PM}_{2.5}$ concentrations were 82, 57, 52, 65, and 47 $\mu\text{g m}^{-3}$, respectively. The relative error (RE) between the observed mean $\text{PM}_{2.5}$ concentrations and the CV-predicted mean $\text{PM}_{2.5}$ concentrations ranged from -17 to 15% , with a mean RE of -5% . The RMSE of the RE was 14.6% , reflecting the uncertainties of the GLM method in quantitatively estimating the contribution of the meteorological conditions to the air pollutant concentrations.

Table 5 also lists the daily RMSE for each CV period and the total RMSE. The daily RMSE for each CV period was calculated with the daily average $\text{PM}_{2.5}$ concentrations during each CV period, and the total RMSE was calculated with the daily average $\text{PM}_{2.5}$ concentration throughout all five CV periods combined. The daily RMSE ranged from 19 to 53 $\mu\text{g m}^{-3}$, and the total RMSE was 33 $\mu\text{g m}^{-3}$, indicating that the model prediction accuracy at the daily level needs to be improved. Liu et al. (2012) used a generalized additive model (GAM) to predict $\text{PM}_{2.5}$, which had a total daily RMSE of 23 $\mu\text{g m}^{-3}$. Compared with their results, the CV performance in our study was satisfactory considering that the independent variables in our model were only based on meteorological parameters, while the model of Liu et al. (2012) included AOD.

The RE calculated with the CV method for GLM was -5% (Table 5), which was smaller than the mean percentage difference (-16%) calculated based on days with stable meteorological conditions (Table S7). Moreover, the RMSE of RE calculated with the CV method for GLM (Table 5) was 14.6% , which was also smaller than the RMSE of percentage difference (18%) calculated based on days with stable meteorological conditions (Table S7).

These indicate that the GLM reduced uncertainties of the method in quantitatively estimating the contribution of the meteorological conditions to the pollutant concentrations.

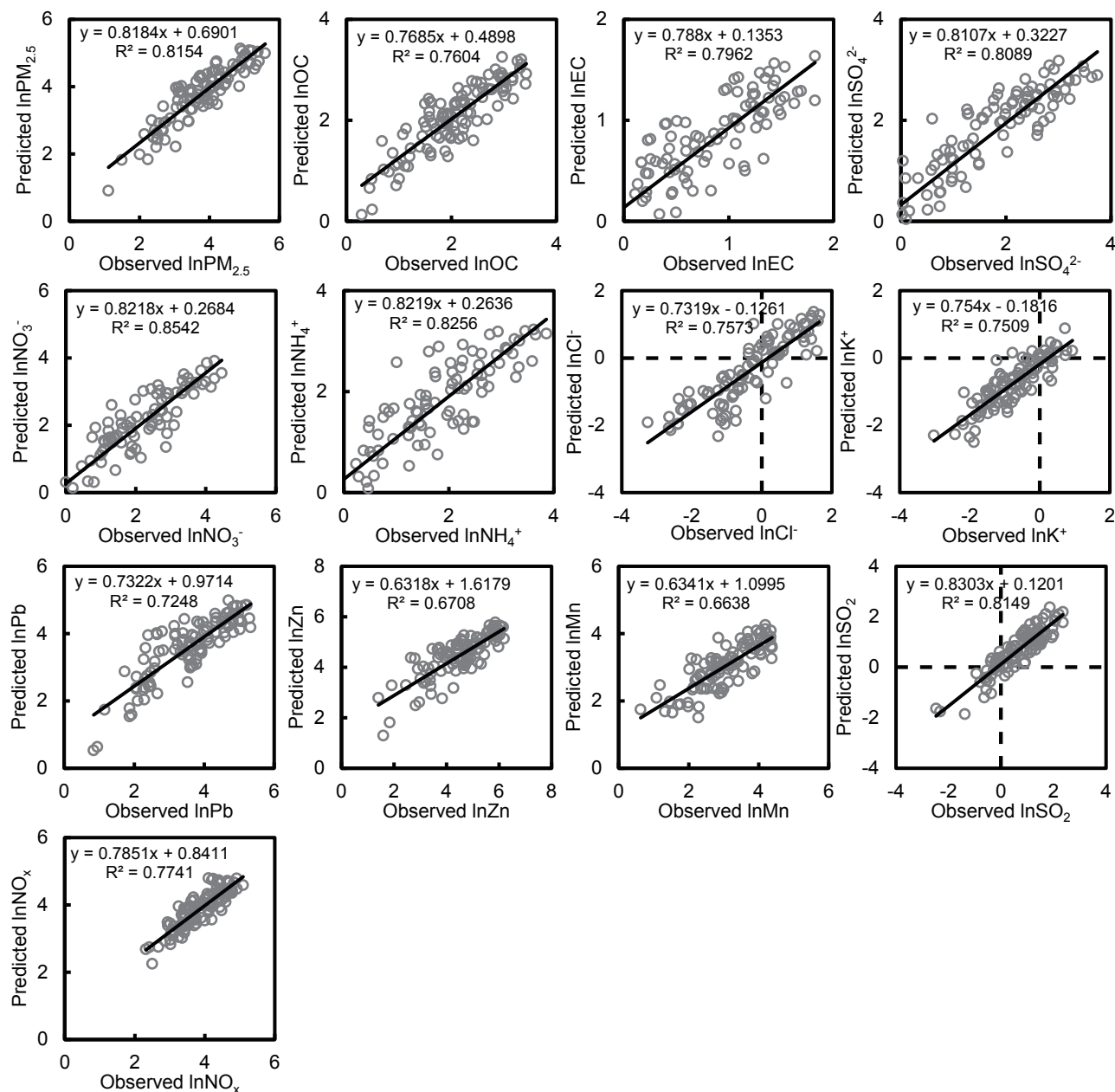


Figure 7. Scatter plot and correlations between GLM-predicted (y axis) and observed (x axis) concentrations of pollutants transformed to a natural log. The linear regression equations and R^2 values are given.

3.3.2 Model description

Table 6 shows the concentrations of air pollutants for the GLM with adjusted R^2 values higher than 0.6. The adjusted R^2 of the $PM_{2.5}$, NO_3^- , NH_4^+ , and SO_2 models are higher than 0.8, indicating that these models could explain more than 80% of the variation in air pollutant concentrations.

Again, we used the $PM_{2.5}$ model as an example. Table 7 lists the output indexes of the $PM_{2.5}$ GLM, including a model summary, analysis of variance (ANOVA), coefficients, and

other indexes. The values of R , R^2 , and adjusted R^2 were 0.910, 0.828, and 0.808, respectively, indicating that the $PM_{2.5}$ model can explain 80.8% of the variability of the daily average $PM_{2.5}$ concentrations. The model was statistically significant according to the p value (< 0.05) from an F test, and the meteorological parameters eventually selected as the independent variables of the model were statistically significant according to the p values (< 0.05) from a t test. The meteorological parameters eventually included in the model were $\ln WS$, $\ln WS_{\max(\text{lag})}$, PBL_{\max} , $PREC$, $\ln \Delta T_{(\text{lag})}$,

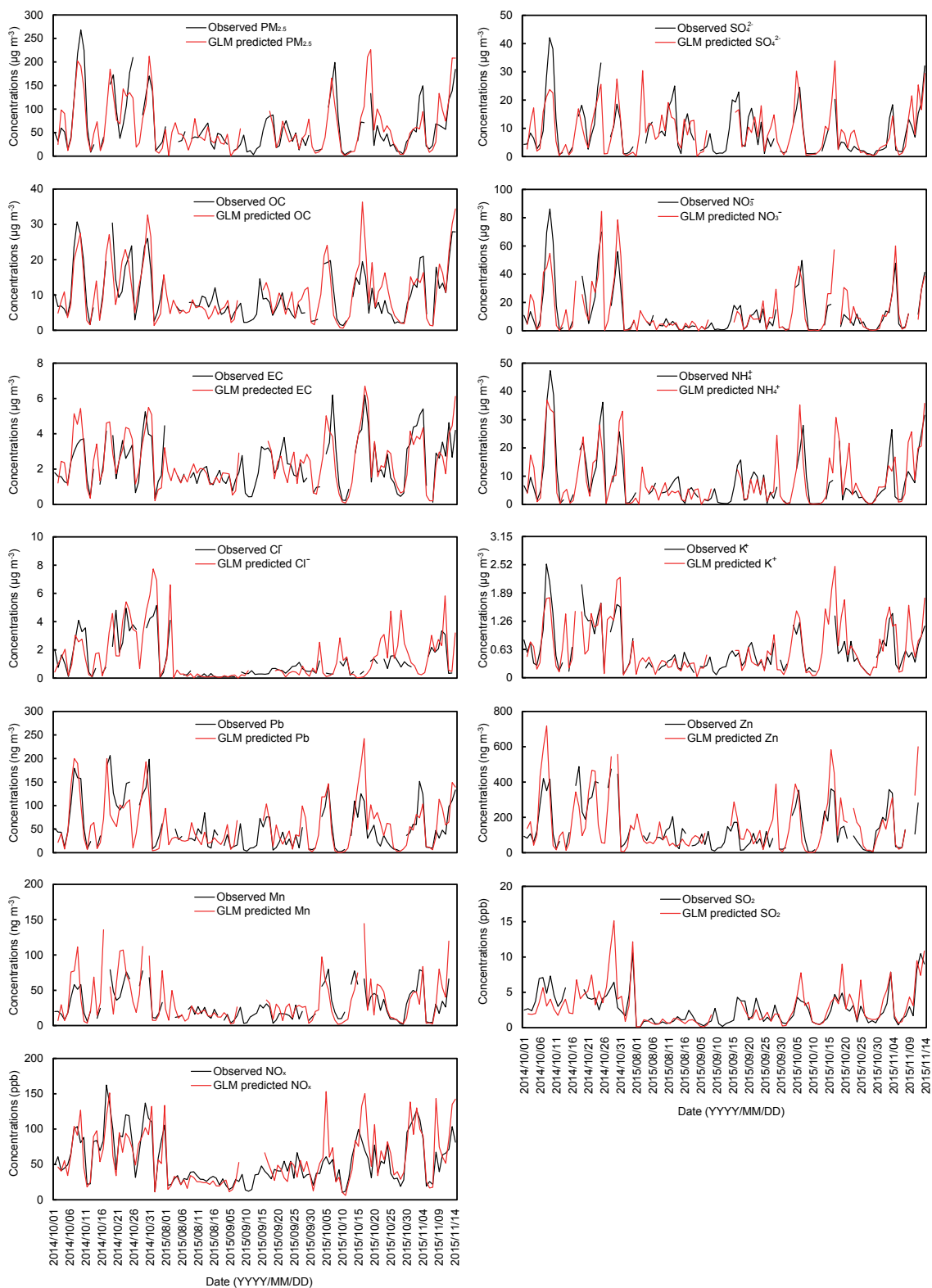


Figure 8. Time series of the observed (in black line) and GLM-predicted pollutant concentrations (in red line).

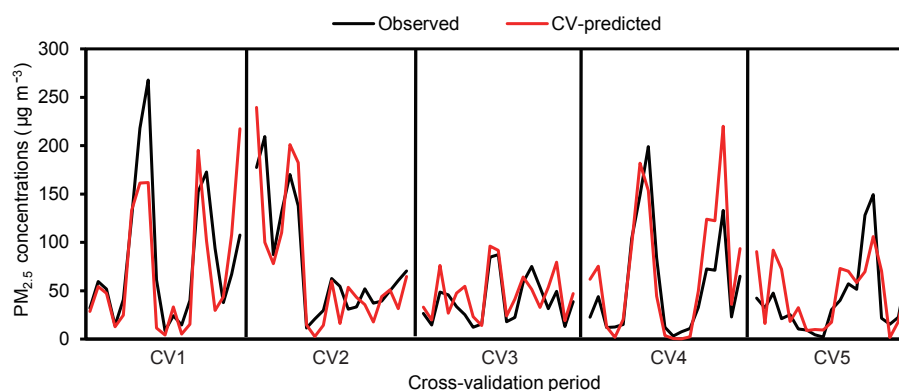


Figure 9. Time series of the observed and cross-validation (CV) predicted $\text{PM}_{2.5}$ concentrations during five CV periods. The black line represents the observed $\text{PM}_{2.5}$ concentration and the red line represents the CV-predicted $\text{PM}_{2.5}$ concentration.

WS_{mode} , $\text{WD}/\text{WS}_{(\text{lag})}$, $\text{PBL}_{\text{min}(\text{lag})}$, $\text{PREC}_{(\text{lag})}$, and SLP_{min} . According to the collinearity statistics, all the VIF values were within 5 and tolerance values were larger than 0.1, indicating that no serious multicollinearity existed between the independent parameters. The Durbin–Watson value (1.910) was close to 2, accounting for the good independence of the variance. Figure S9 shows the graphic residual analysis of the $\text{PM}_{2.5}$ GLM.

Table 8 summarizes the meteorological parameters included in the models and their influence on pollutant concentrations. As a result, PBL, $\text{WS}_{(\text{lag})}$, $\text{PREC}_{(\text{lag})}$, PREC, and WS are included in the models more frequently, accounting for 13, 9, 8, 7, and 7 times. This indicates that these parameters have important influence on pollutant concentrations, especially for PBL included in all of the models. The parameters of the previous day also have important influence on pollutant concentrations, i.e., $\text{WS}_{(\text{lag})}$, $\text{PREC}_{(\text{lag})}$, $\text{PBL}_{(\text{lag})}$, $\text{RH}_{(\text{lag})}$, $T_{(\text{lag})}$, $\text{WD}/\text{WS}_{(\text{lag})}$, and $\text{WD}_{(\text{lag})}$. Meteorological parameters have different influence on pollutant concentrations (Table 8). For example, PBL, $\text{WS}_{(\text{lag})}$, and $\text{PREC}_{(\text{lag})}$ represent the negative correlation with pollutant concentrations. This may be because the higher values of these meteorological parameters are in favor of pollution diffusion. On the contrary, RH, T , $\text{WD}/\text{WS}_{(\text{lag})}$, and WD represent the positive correlation with pollutant concentrations, because the higher values of these meteorological parameters are beneficial for pollution formation and accumulation.

3.3.3 Quantitative estimates of the contribution of meteorological conditions to air pollutant concentrations

We applied the GLM to predict air pollutant concentrations during APEC 2014 and Victory Parade 2015 based on meteorological parameters. The difference between the observed and GLM-predicted concentrations was attributed to emission reduction through the implementation of air pollution control strategies.

Table 9 lists the percentage differences between the observed and GLM-predicted concentrations of air pollutants during APEC and the Victory Parade. The mean concentrations of the observed and predicted $\text{PM}_{2.5}$ were 48 and $67 \mu\text{g m}^{-3}$ during APEC, i.e., a 28 % difference. The mean concentrations of the observed and predicted $\text{PM}_{2.5}$ were 15 and $20 \mu\text{g m}^{-3}$ during the parade, i.e., a 25 % difference. These differences are attributed to the emission reduction through the implementation of air pollution control strategies. As described in Sect. 3.1, during APEC and the parade, the mean concentrations of $\text{PM}_{2.5}$ decreased by 58 and 63 % compared with before APEC and the parade. Therefore, the meteorological conditions and pollution control strategies contributed 30 and 28 % to the reduction of the $\text{PM}_{2.5}$ concentration during APEC 2014 and 38 and 25 % during the Victory Parade 2015, respectively, based on the assumption that the concentrations of air pollutants are only determined by meteorological conditions and emission intensities.

The emission reduction during APEC in this study is comparable to the results of other studies where meteorological influences were considered. For example, the $\text{PM}_{2.5}$ concentration decreased by 33 % under the same weather conditions during APEC in Beijing as modeled by the Weather Research and Forecasting model and Community Multiscale Air Quality (WRF/CMAQ) model (Wu et al., 2015). In addition, emission control implemented in Beijing during APEC resulted in a 22 % reduction in the $\text{PM}_{2.5}$ concentration, as modeled by WRF-Chem (Guo et al., 2016).

Same as $\text{PM}_{2.5}$, the differences listed in Table 9 for other pollutants show the reduction in emission of these pollutants and/or their precursors. The differences for EC were 37 % (from 2.7 to $1.7 \mu\text{g m}^{-3}$) during APEC and 33 % (from 1.2 to $0.8 \mu\text{g m}^{-3}$) during the parade. In contrast, the differences for OC were 11 % (from 12.6 to $11.2 \mu\text{g m}^{-3}$) during APEC and 8 % (from 3.7 to $4.0 \mu\text{g m}^{-3}$) during the parade. The differences for carbonaceous components (OC + EC) were 16 % (from 15.3 to $12.9 \mu\text{g m}^{-3}$) during APEC and 2 % (from 4.9 to $4.8 \mu\text{g m}^{-3}$) during the parade. This indicates that the

Table 6. The concentrations of air pollutants for the GLM with adjusted R^2 values higher than 0.6.

Pollutants	Model descriptions	Adjusted R^2
PM _{2.5}	$\ln(\text{PM}_{2.5}) = -0.48 \ln \text{WS} - 0.43 \ln \text{WS}_{\text{max}(\text{lag})} - 0.00076 \text{PBL}_{\text{max}} - 0.11 \text{PREC} + 0.25 \ln \Delta T_{(\text{lag})} - 0.14 \text{WS}_{\text{mode}} + 0.48 \text{WD}/\text{WS}_{(\text{lag})} + 0.0043 \text{PBL}_{\text{min}(\text{lag})} - 0.025 \text{PREC}_{(\text{lag})} - 0.015 \text{SLP}_{\text{min}} + 19.51$	0.808
EC	$\ln(\text{EC}) = 0.60 \ln \text{WD}/\text{WS}_{\text{sum}} - 0.59 \ln \text{PBL} - 0.017 \text{PREC}_{(\text{lag})} + 0.22 \ln \Delta T - 0.50 \ln \text{WS}_{(\text{lag})} + 0.25 \ln \text{PBL}_{\text{max}(\text{lag})} - 0.17$	0.780
OC	$\ln(\text{OC}) = -0.44 \ln \text{WS} + 0.47 \text{WD}/\text{WS}_{(\text{lag})} - 0.67 \ln \text{PBL} - 0.020 \text{PREC}_{(\text{lag})} + 0.67 \ln \text{WD} + 0.17 \ln \Delta T - 0.65 \ln \text{RH}_{\text{max}(\text{lag})} + 7.84$	0.751
SO ₄ ²⁻	$\ln(\text{SO}_4^{2-}) = -0.99 \ln \text{WS}_{(\text{lag})} + 0.066 T_{\text{min}} - 0.040 \text{PREC}_{(\text{lag})} - 1.20 \ln \text{PBL} + 0.0011 \text{PBL}_{(\text{lag})} + 0.019 \text{RH} - 0.12 \text{PREC} + 0.087 \text{WS}_{\text{max}} + 6.68$	0.795
NO ₃ ⁻	$\ln(\text{NO}_3^-) = -1.90 \ln \text{PBL} - 0.96 \ln \text{WS}_{(\text{lag})} + 0.88 \text{WD} + 0.0045 \text{PBL}_{\text{min}} - 0.20 \text{PREC} + 0.12 \text{WS}_{\text{max}} + 1.57 \ln \text{RH} + 0.60 \ln \Delta T_{(\text{lag})} - 1.22 \ln \text{RH}_{\text{max}(\text{lag})} - 0.047 \Delta T + 9.32$	0.833
NH ₄ ⁺	$\ln(\text{NH}_4^+) = 0.040 \text{RH} - 1.27 \ln \text{WS}_{(\text{lag})} - 1.03 \ln \text{RH}_{(\text{lag})} - 0.00075 \text{PBL}_{\text{max}} - 0.16 \text{PREC} + 0.33 \ln \Delta T_{(\text{lag})} + 4.28$	0.813
Cl ⁻	$\ln(\text{Cl}^-) = -1.12 \ln \text{PBL} - 0.072 T_{(\text{lag})} + 1.60 \ln \text{WD} - 2.32 \ln \text{RH}_{\text{max}(\text{lag})} + 0.53 \ln \text{WD}/\text{WS}_{\text{sum}(\text{lag})} + 14.69$	0.737
K ⁺	$\ln(\text{K}^+) = -0.75 \ln \text{PBL} - 0.66 \ln \text{WS}_{(\text{lag})} - 0.020 \text{RH}_{(\text{lag})} + 0.0056 \text{PBL}_{\text{min}} - 0.20 \text{WS}_{\text{mode}} + 0.33 \ln \Delta T_{(\text{lag})} - 0.47 \ln \text{PBL}_{\text{max}(\text{lag})} - 0.087 \text{PREC} + 0.66 \ln \text{RH} + 5.46$	0.717
Pb	$\ln(\text{Pb}) = -0.61 \ln \text{WS} - 0.67 \ln \text{WS}_{\text{max}(\text{lag})} + 0.36 \ln \Delta T_{(\text{lag})} - 0.00062 \text{PBL}_{\text{max}} - 0.19 \text{WS}_{\text{mode}} - 0.030 \text{PREC}_{(\text{lag})} + 5.39$	0.721
Zn	$\ln(\text{Zn}) = -0.81 \ln \text{WS} - 0.41 \ln \text{WS}_{\text{max}(\text{lag})} - 0.0016 \text{PBL} - 0.36 \ln \text{WS}_{\text{mode}(\text{lag})} + 6.56$	0.627
Mn	$\ln(\text{Mn}) = 0.80 \text{WD}/\text{WS} - 0.98 \ln \text{PBL} - 0.043 \text{PREC}_{(\text{lag})} + 0.57 \text{WD}/\text{WS}_{(\text{lag})} - 0.017 \text{RH} - 0.023 \text{SLP} + 0.0030 \text{PBL}_{\text{min}(\text{lag})} + 31.04$	0.656
SO ₂	$\ln(\text{SO}_2) = -1.32 \ln \text{PBL} - 0.071 \text{PREC}_{(\text{lag})} - 0.047 \text{PREC} + 0.29 \text{WD}_{\text{mode}(\text{lag})} - 0.026 \text{RH} - 0.47 \ln \text{WS}_{(\text{lag})} + 14.12 \ln \text{SLP}_{\text{max}} - 87.56$	0.803
NO _x	$\ln(\text{NO}_x) = 0.014 \text{WD}/\text{WS}_{\text{sum}} - 0.030 T_{\text{min}} + 0.27 \ln \Delta T - 0.44 \ln \text{PBL} - 0.015 \text{PREC} - 0.012 \text{PREC}_{(\text{lag})} + 5.30$	0.772

emission reductions for OC and its precursors were smaller than the reduction of EC during APEC and the parade. This may be because OC can originate from both primary emission and secondary transformation. The slope of the OC/EC correlation during the pollution control period reached 6.86 (Fig. 3), indicating the higher levels of SOC formation during the control periods.

Table 9 also shows the differences for sulfate were 44 % (from 2.7 to 3.9 $\mu\text{g m}^{-3}$) during APEC and 50 % (from 5.2 to 2.6 $\mu\text{g m}^{-3}$) during the parade. The differences for nitrate were 44 % (from 19.0 to 10.6 $\mu\text{g m}^{-3}$) during APEC and

56 % (from 3.4 to 1.5 $\mu\text{g m}^{-3}$) during the parade. The differences for ammonium were 13 % (from 5.5 to 4.8 $\mu\text{g m}^{-3}$) during APEC and 38 % (from 2.4 to 1.5 $\mu\text{g m}^{-3}$) during the parade. In total, the differences for SNA were 29 % (from 27.2 to 19.3 $\mu\text{g m}^{-3}$) during APEC and 49 % (from 11.0 to 5.6 $\mu\text{g m}^{-3}$) during the parade. The control of the SNA concentration was very effective during APEC and the parade, leading to a significant decrease of PM_{2.5} during both events. The significant differences for sulfate and nitrate may indicate the control of coal combustion and/or vehicle emission were effective during APEC and the parade.

Table 7. The output indexes of the PM_{2.5} GLM, including a model summary, analysis of variance (ANOVA), coefficients, and other indexes.

Model summary and ANOVA						
<i>R</i>	<i>R</i> ²	Adjusted <i>R</i> ²	SE of the estimate	Durbin–Watson	<i>F</i>	Sig.*
0.910	0.828	0.808	0.411	1.910	41.763	0.000
Coefficients						
Model	Unstandardized coefficients		<i>t</i>	Sig. ^a	Collinearity statistics	
	<i>B</i>	SE			Tolerance	VIF
(Constant)	19.512	6.871	2.840	0.006		
lnWS	−0.483	0.162	−2.971	0.004	0.313	3.194
lnWS _{max(lag)}	−0.431	0.153	−2.818	0.006	0.300	3.331
PBL _{max}	−0.001	0.000	−6.747	0.000	0.395	2.534
PREC	−0.110	0.029	−3.735	0.000	0.618	1.618
ln Δ <i>T</i> _(lag)	0.247	0.083	2.975	0.004	0.662	1.512
WS _{mode}	−0.135	0.050	−2.726	0.008	0.493	2.027
WD/WS _(lag)	0.476	0.148	3.222	0.002	0.353	2.829
PBL _{min(lag)}	0.004	0.001	3.510	0.001	0.407	2.459
PREC _(lag)	−0.025	0.009	−2.796	0.006	0.707	1.415
SLP _{min}	−0.015	0.007	−2.176	0.032	0.707	1.414

* The significance level is 0.05.

Table 8. The influence of the meteorological parameters included in the GLMs on pollutant concentrations¹.

Parameters	Included in the GLM (times) ²	PM _{2.5}	EC	OC	SO ₄ ^{2−}	NO ₃ [−]	NH ₄ ⁺	Cl [−]	K ⁺	Pb	Zn	Mn	SO ₂	NO _x
PBL	13	−	−	−	−	+−	−	−	+−	−	−	−	−	−
WS _(lag)	9	−	−	−	−	−	−	−	−	−	−	−	−	−
PREC _(lag)	8	−	−	−	−	−	−	−	−	−	−	−	−	−
PREC	7	−	−	−	−	−	−	−	−	−	−	−	−	−
WS	7	−	−	−	+	+	−	−	−	−	−	−	−	−
RH	6	−	−	−	+	+	+	+	−	−	−	−	−	−
PBL _(lag)	5	+	+	−	+	−	−	−	−	−	−	+	−	−
RH _(lag)	5	−	−	−	−	−	−	−	−	−	−	−	−	−
T	5	−	−	−	+	+	+	−	−	−	−	−	−	−
<i>T</i> _(lag)	5	+	−	−	−	−	−	−	+	+	−	−	−	−
WD/WS _(lag)	4	+	−	−	+	−	−	−	−	−	−	−	−	−
SLP	3	−	−	−	−	−	−	−	−	−	−	−	+	−
WD	3	−	−	−	−	−	−	−	−	−	−	−	−	−
WD/WS	3	−	−	−	−	−	−	−	−	−	−	−	−	−
WD _(lag)	1	−	−	−	−	−	−	−	−	−	−	−	−	−

¹ + represents the positive correlation, and − represents the negative correlation between meteorological parameters and pollutant concentrations.

² If a parameter is included in the model for several times, it will be counted as one time.

The concentration of sulfate is determined by primary emissions and secondary transformation from SO₂; thus, the changes in sulfate concentrations may not reflect well the effectiveness of emission control strategies. One needs to also include the changes in SO₂ concentrations. By adding the molar concentrations of SO₂ and SO₄^{2−} ($S = [\text{SO}_2] + [\text{SO}_4^{2-}]$), the concentration of total S was calculated. Table 9 shows the differences for SO₂ were 50 %

(from 6.59 to 3.32 ppb) during APEC and 2 % (from 0.56 to 0.57 ppb) during the parade, while the differences for total S were 41 % (from 0.322 to 0.189 μmol m^{−3}) during APEC and 33 % (from 0.079 to 0.053 μmol m^{−3}) during the parade. Coal combustion emissions is the major contributor to total S, this demonstrates the effective control of coal combustion during both APEC 2014 and the Victory Parade 2015. The difference for SO₂ during APEC was larger than that

Table 9. The percentage differences between the observed and GLM-predicted concentrations of the air pollutants during APEC and the Victory Parade.

Pollutants	Units	During APEC			During parade		
		Observed	Predicted	Percentage differences ¹	Observed	Predicted	Percentage differences ¹
PM _{2.5}	μg m ⁻³	48	67	28 %	15	20	25 %
OC		11.2	12.6	11 %	4.0	3.7	-8 %
EC		1.7	2.7	37 %	0.8	1.2	33 %
SO ₄ ²⁻		3.9	2.7	-44 %	2.6	5.2	50 %
NO ₃ ⁻		10.6	19.0	44 %	1.5	3.4	56 %
NH ₄ ⁺		4.8	5.5	13 %	1.5	2.4	38 %
Cl ⁻		2.06	2.58	20 %	0.16	0.17	6 %
K ⁺		0.65	1.03	37 %	0.18	0.24	25 %
Pb	ng m ⁻³	55	70	21 %	9	17	47 %
Zn		128	171	25 %	20	41	51 %
Mn		34.5	51.5	33 %	3.6	7.6	53 %
SO ₂	ppb	3.32	6.59	50 %	0.57	0.56	-2 %
NO _x		45	102	56 %	13	20	35 %
OC + EC	μg m ⁻³	12.9	15.3	16 %	4.8	4.9	2 %
SNA	μg m ⁻³	19.3	27.2	29 %	5.6	11.0	49 %
total S ²	μmol m ⁻³	0.189	0.322	41 %	0.053	0.079	33 %

¹ Percentage difference = (predicted - observed) / predicted × 100 %.

² Total S = [SO₂] + [SO₄²⁻].

during the parade, while the difference for sulfate during the parade was larger than that during APEC. As discussed in Sect. 3.1, the mean SOR was 27 and 64 % during APEC and the parade, respectively, indicating that the SO₂-to-sulfate transformation rate during APEC (autumn and early winter) was much lower than during the parade (late summer and autumn).

Table 9 shows NO_x and other PM_{2.5} components also had significant emission reduction during APEC 2014 and the Victory Parade 2015. The differences between the observed and GLM-predicted concentrations of NO_x were 56 % (from 102 to 45 ppb) during APEC and 35 % (from 20 to 13 ppb) during the parade. The differences for Cl⁻ were 20 % (from 2.58 to 2.06 μg m⁻³) during APEC and 6 % (from 0.17 to 0.16 μg m⁻³) during the parade. The differences for K⁺ were 37 % (from 1.03 to 0.65 μg m⁻³) during APEC and 25 % (from 0.24 to 0.18 μg m⁻³) during the parade. The differences for Pb, Zn, and Mn ranged from 21 to 53 % during APEC and the parade. The concentrations of Cl⁻ have been found to be high in the fine particles produced from coal combustion (Takuwa et al., 2006), while the concentrations of K⁺ are high in particles derived from combustion activities, e.g., biomass burning and coal combustion. Lead is typically considered to be a marker of emissions from coal combustion, power stations, and metallurgical plants (Dan et al., 2004; Mukai et al., 2001; Schleicher et al., 2011). Zinc can be produced by the action of a car braking and by tire

wear (Cyrus et al., 2003; Sternbeck et al., 2002). Manganese mainly originates from industrial activities. Major sources of NO_x emissions include power plants, industry, and transportation (Liu and Zhu, 2013). The differences for the concentrations of total S, Cl⁻, K⁺, Pb, Zn, Mn, and NO_x indicate that the control of anthropogenic emissions, especially coal combustion, was very effective during APEC and the parade.

3.3.4 Uncertainties of the GLM

In this study, the uncertainties of the GLM when estimating the contributions of meteorological conditions and pollution control strategies in reducing air pollution were assessed with the CV test (Table 5) in Sect. 3.3.1. All GLMs were developed following the same procedure; thus the PM_{2.5} model was used as an example representative of all the pollutants. As a result, the relative errors between the observed mean PM_{2.5} concentrations and the CV-predicted mean PM_{2.5} concentrations were within ±20 %, averaging with -5 %. This indicates that the PM_{2.5} concentrations could be predicted with the GLM based on the meteorological conditions. The uncertainties of the GLM could refer to the RMSE of RE for GLM of 14.6 % (Table 5). It should be mentioned that the data input to the PM_{2.5} model was allocated randomly into several periods, and thus the RMSE of RE for GLM would vary accordingly. In the future, we could test the uncertainties of the GLMs for other pollutants with the CV test.

4 Conclusions

During the pollution control periods of APEC 2014 and the Victory Parade 2015, the concentrations of air pollutants except ozone decreased dramatically compared with the concentrations during non-control periods, accompanied by meteorological conditions favorable for pollutant dispersal.

To estimate the contributions of meteorological conditions and pollution control strategies in reducing air pollution, comparing the concentrations of air pollutants during days with stable meteorological conditions is a useful method but has limitations due to high uncertainty and lack of a sufficient number of days with stable meteorological conditions.

Our study shows that, if including the nonlinear relationship between meteorological parameters and air pollutant concentrations, GLMs based only on meteorological parameters could provide a good explanation of the variation of pollutant concentrations, with adjusted R^2 values mostly larger than 0.7. Since the GLMs contained no parameters dependent on air pollution levels as independent variables, they could be used to estimate the contributions of meteorological conditions and pollution control strategies to the air pollution levels during emission control periods.

With the GLMs method, we found meteorological conditions and pollution control strategies played almost equally important roles in reducing air pollution in megacity Beijing during APEC 2014 and the Victory Parade 2015, e.g., 30 and 28 % reduction of the $PM_{2.5}$ concentration during APEC 2014 as well as 38 and 25 % during the Victory Parade 2015. We also found that the control of the SNA concentration was more effective than carbonaceous components. The differences between the observed and GLM-predicted concentrations of specific pollutants (Cl^- , K^+ , Pb, Zn, Mn, NO_x , and S) related to coal combustion and industrial activities revealed the effective control of anthropogenic emissions.

In the future, by combining the methods of source apportionment, the contributions of emission reductions for different sources in reducing air pollution could be estimated, enabling further analysis of pollution control strategies.

Data availability. The data of stationary measurements are available upon requests.

The Supplement related to this article is available online at <https://doi.org/10.5194/acp-17-13921-2017-supplement>.

Author contributions. TZ and PFL designed the experiments. PFL collected and weighed the $PM_{2.5}$ filter samples. PFL, YHF, YQH, and JXW carried out the analysis of the components in $PM_{2.5}$. YSW and MH provided the data of gaseous pollutant concentrations. YRL computed the data of planetary boundary layer heights from GDAS and PFL developed the GLM. JXW managed the data. PFL ana-

lyzed the data with contributions from all coauthors. PFL prepared the manuscript with help from TZ.

Competing interests. The authors declare that they have no conflict of interest.

Special issue statement. This article is part of the special issue “Regional transport and transformation of air pollution in eastern China”. It is not associated with a conference.

Acknowledgements. This study was supported by the National Natural Science Foundation Committee of China (41421064, 21190051), the European 7th Framework Programme Project PURGE (265325), and the Collaborative Innovation Center for Regional Environmental Quality.

Edited by: Jianmin Chen

Reviewed by: two anonymous referees

References

- Barnpadimos, I., Keller, J., Oderbolz, D., Hueglin, C., and Prévôt, A. S. H.: One decade of parallel fine ($PM_{2.5}$) and coarse ($PM_{10-PM_{2.5}}$) particulate matter measurements in Europe: trends and variability, *Atmos. Chem. Phys.*, 12, 3189–3203, <https://doi.org/10.5194/acp-12-3189-2012>, 2012.
- Calkins, C., Ge, C., Wang, J., Anderson, M., and Yang, K.: Effects of meteorological conditions on sulfur dioxide air pollution in the North China Plain during winters of 2006–2015, *Atmos. Environ.*, 147, 296–309, <https://doi.org/10.1016/j.atmosenv.2016.10.005>, 2016.
- CEPB: Chengdu Environmental Protection Bureau, available at: <http://www.cdepb.gov.cn/cdepbws/Web/Template/GovDefaultInfo.aspx?cid=236&aid=22738>, last access: 25 May 2017, (in Chinese), 2013.
- China, S. C. o.: State Council of P. R. China’s notification on Action Plan for Air Pollution Prevention and Control, available at: http://www.gov.cn/zw/gk/2013-09/12/content_2486773.htm, last access: 12 September 2013 (in Chinese).
- Chitranshi, S., Sharma, S. P., and Dey, S.: Spatio-temporal variations in the estimation of PM_{10} from MODIS-derived aerosol optical depth for the urban areas in the Central Indo-Gangetic Plain, *Meteorol. Atmos. Phys.*, 127, 107–121, <https://doi.org/10.1007/s00703-014-0347-z>, 2015.
- Chow, J. C., Watson, J. G., Lu, Z. Q., Lowenthal, D. H., Frazier, C. A., Solomon, P. A., Thuillier, R. H., and Magliano, K.: Descriptive analysis of $PM_{2.5}$ and PM_{10} at regionally representative locations during SJVAQS/AUSPEX, *Atmos. Environ.*, 30, 2079–2112, [https://doi.org/10.1016/1352-2310\(95\)00402-5](https://doi.org/10.1016/1352-2310(95)00402-5), 1996.
- Chudnovsky, A. A., Koutrakis, P., Kloog, I., Melly, S., Nordio, F., Lyapustin, A., Wang, Y. J., and Schwartz, J.: Fine particulate matter predictions using high resolution Aerosol Optical Depth (AOD) retrievals, *Atmos. Environ.*, 89, 189–198, <https://doi.org/10.1016/j.atmosenv.2014.02.019>, 2014.

- Cyrys, J., Heinrich, J., Hoek, G., Meliefste, K., Lewne, M., Gehring, U., Bellander, T., Fischer, P., Van Vliet, P., Brauer, M., Wichmann, H. E., and Brunekreef, B.: Comparison between different traffic-related particle indicators: Elemental carbon (EC), PM_{2.5} mass, and absorbance, *J. Expo. Anal. Env. Epidemiol.*, 13, 134–143, <https://doi.org/10.1038/sj.jea.7500262>, 2003.
- Dan, M., Zhuang, G. S., Li, X. X., Tao, H. R., and Zhuang, Y. H.: The characteristics of carbonaceous species and their sources in PM_{2.5} in Beijing, *Atmos. Environ.*, 38, 3443–3452, <https://doi.org/10.1016/j.atmosenv.2004.02.052>, 2004.
- Diaz-Robles, L. A., Ortega, J. C., Fu, J. S., Reed, G. D., Chow, J. C., Watson, J. G., and Moncada-Herrera, J. A.: A hybrid ARIMA and artificial neural networks model to forecast particulate matter in urban areas: the case of Temuco, Chile, *Atmos. Environ.*, 42, 8331–8340, <https://doi.org/10.1016/j.atmosenv.2008.07.020>, 2008.
- GEPB: Guangzhou Environmental Protection Bureau, available at: <http://www.gz.gov.cn/gzgov/s2812/200912/163197.shtml>, last access: 25 May 2017, (in Chinese), 2009.
- Guo, J. P., He, J., Liu, H. L., Miao, Y. C., Liu, H., and Zhai, P. M.: Impact of various emission control schemes on air quality using WRF-Chem during APEC China 2014, *Atmos. Environ.*, 140, 311–319, <https://doi.org/10.1016/j.atmosenv.2016.05.046>, 2016.
- Gupta, P. and Christopher, S. A.: Particulate matter air quality assessment using integrated surface, satellite, and meteorological products: Multiple regression approach, *J. Geophys. Res.*, 114, 13, <https://doi.org/10.1029/2008jd011496>, 2009.
- Han, T. T., Xu, W. Q., Chen, C., Liu, X. G., Wang, Q. Q., Li, J., Zhao, X. J., Du, W., Wang, Z. F., and Sun, Y. L.: Chemical apportionment of aerosol optical properties during the Asia-Pacific Economic Cooperation summit in Beijing, China, *J. Geophys. Res.*, 120, 12281–12295, <https://doi.org/10.1002/2015JD023918>, 2015.
- Hien, P. D., Bac, V. T., Tham, H. C., Nhan, D. D., and Vinh, L. D.: Influence of meteorological conditions on PM_{2.5} and PM_{2.5–10} concentrations during the monsoon season in Hanoi, Vietnam, *Atmos. Environ.*, 36, 3473–3484, [https://doi.org/10.1016/S1352-2310\(02\)00295-9](https://doi.org/10.1016/S1352-2310(02)00295-9), 2002.
- Huang, X.-F., He, L.-Y., Hu, M., Canagaratna, M. R., Sun, Y., Zhang, Q., Zhu, T., Xue, L., Zeng, L.-W., Liu, X.-G., Zhang, Y.-H., Jayne, J. T., Ng, N. L., and Worsnop, D. R.: Highly time-resolved chemical characterization of atmospheric submicron particles during 2008 Beijing Olympic Games using an Aerodyne High-Resolution Aerosol Mass Spectrometer, *Atmos. Chem. Phys.*, 10, 8933–8945, <https://doi.org/10.5194/acp-10-8933-2010>, 2010.
- Huang, X.-F., He, L.-Y., Xue, L., Sun, T.-L., Zeng, L.-W., Gong, Z.-H., Hu, M., and Zhu, T.: Highly time-resolved chemical characterization of atmospheric fine particles during 2010 Shanghai World Expo, *Atmos. Chem. Phys.*, 12, 4897–4907, <https://doi.org/10.5194/acp-12-4897-2012>, 2012.
- Kelly, F. J. and Zhu, T.: Transport solutions for cleaner air, *Science*, 352, 934–936, <https://doi.org/10.1126/science.aaf3420>, 2016.
- Li, H., Zhang, Q., Zhang, Q., Chen, C., Wang, L., Wei, Z., Zhou, S., Parworth, C., Zheng, B., Canonaco, F., Prévôt, A. S. H., Chen, P., Zhang, H., Wallington, T. J., and He, K.: Wintertime aerosol chemistry and haze evolution in an extremely polluted city of the North China Plain: significant contribution from coal and biomass combustion, *Atmos. Chem. Phys.*, 17, 4751–4768, <https://doi.org/10.5194/acp-17-4751-2017>, 2017.
- Liu, H., Wang, X. M., Zhang, J. P., He, K. B., Wu, Y., and Xu, J. Y.: Emission controls and changes in air quality in Guangzhou during the Asian Games, *Atmos. Environ.*, 76, 81–93, <https://doi.org/10.1016/j.atmosenv.2012.08.004>, 2013.
- Liu, J. and Zhu, T.: NO_x in Chinese Megacities, *Nato. Sci. Peace Secur.*, 120, 249–263, https://doi.org/10.1007/978-94-007-5034-0_20, 2013.
- Liu, J., Mauzerall, D. L., Chen, Q., Zhang, Q., Song, Y., Peng, W., Klimont, Z., Qiu, X. H., Zhang, S. Q., Hu, M., Lin, W. L., Smith, K. R., and Zhu, T.: Air pollutant emissions from Chinese households: a major and underappreciated ambient pollution source, *P. Natl. Acad. Sci. USA*, 113, 7756–7761, <https://doi.org/10.1073/pnas.1604537113>, 2016.
- Liu, W., Li, X. D., Chen, Z., Zeng, G. M., Leon, T., Liang, J., Huang, G. H., Gao, Z. H., Jiao, S., He, X. X., and Lai, M. Y.: Land use regression models coupled with meteorology to model spatial and temporal variability of NO₂ and PM₁₀ in Changsha, China, *Atmos. Environ.*, 116, 272–280, <https://doi.org/10.1016/j.atmosenv.2015.06.056>, 2015.
- Liu, Y., Franklin, M., Kahn, R., and Koutrakis, P.: Using aerosol optical thickness to predict ground-level PM_{2.5} concentrations in the St. Louis area: a comparison between MISR and MODIS, *Remote Sens. Environ.*, 107, 33–44, <https://doi.org/10.1016/j.rse.2006.05.022>, 2007.
- Liu, Y., He, K. B., Li, S. S., Wang, Z. X., Christiani, D. C., and Koutrakis, P.: A statistical model to evaluate the effectiveness of PM_{2.5} emissions control during the Beijing 2008 Olympic Games, *Environ. Int.*, 44, 100–105, <https://doi.org/10.1016/j.envint.2012.02.003>, 2012.
- Mukai, H., Tanaka, A., Fujii, T., Zeng, Y. Q., Hong, Y. T., Tang, J., Guo, S., Xue, H. S., Sun, Z. L., Zhou, J. T., Xue, D. M., Zhao, J., Zhai, G. H., Gu, J. L., and Zhai, P. Y.: Regional characteristics of sulfur and lead isotope ratios in the atmosphere at several Chinese urban sites, *Environ. Sci. Technol.*, 35, 1064–1071, <https://doi.org/10.1021/es001399u>, 2001.
- Nguyen, T. T. N., Bui, H. Q., Pham, H. V., Luu, H. V., Man, C. D., Pham, H. N., Le, H. T., and Nguyen, T. T.: Particulate matter concentration mapping from MODIS satellite data: a Vietnamese case study, *Environ. Res. Lett.*, 10, 095016, <https://doi.org/10.1088/1748-9326/10/9/095016>, 2015.
- NOAA Air Resources Laboratory, available at: <https://ready.arl.noaa.gov/archives.php>, last access: 20 November 2017.
- Raman, R. S. and Kumar, S.: First measurements of ambient aerosol over an ecologically sensitive zone in Central India: relationships between PM_{2.5} mass, its optical properties, and meteorology, *Sci. Total Environ.*, 550, 706–716, <https://doi.org/10.1016/j.scitotenv.2016.01.092>, 2016.
- Richmond-Bryant, J., Saganich, C., Bukiewicz, L., and Kalin, R.: Associations of PM_{2.5} and black carbon concentrations with traffic, idling, background pollution, and meteorology during school dismissals, *Sci. Total Environ.*, 407, 3357–3364, <https://doi.org/10.1016/j.scitotenv.2009.01.046>, 2009.
- Schleicher, N., Norra, S., Dietze, V., Yu, Y., Fricker, M., Kaminski, U., Chen, Y., and Cen, K.: The effect of mitigation measures on size distributed mass concentrations of atmospheric particles and black carbon concentrations during the Olympic Sum-

- mer Games 2008 in Beijing, *Sci. Total Environ.*, 412, 185–193, <https://doi.org/10.1016/j.scitotenv.2011.09.084>, 2011.
- SEPB: Shanghai Environmental Protection Bureau, available at: <http://www.sepb.gov.cn/fa/cms/shhj//shhj2272/shhj2159/2010/02/20671.htm>, last access: 25 May 2017, (in Chinese), 2010.
- Sotoudeheian, S. and Arhami, M.: Estimating ground-level PM₁₀ using satellite remote sensing and ground-based meteorological measurements over Tehran, *J. Environ. Health Sci.*, 12, 122, <https://doi.org/10.1186/S40201-014-0122-6>, 2014.
- Sternbeck, J., Sjodin, A., and Andreasson, K.: Metal emissions from road traffic and the influence of resuspension-results from two tunnel studies, *Atmos. Environ.*, 36, 4735–4744, [https://doi.org/10.1016/S1352-2310\(02\)00561-7](https://doi.org/10.1016/S1352-2310(02)00561-7), 2002.
- Takuwa, T., Mkilaha, I. S. N., and Naruse, I.: Mechanisms of fine particulates formation with alkali metal compounds during coal combustion, *Fuel*, 85, 671–678, <https://doi.org/10.1016/j.fuel.2005.08.043>, 2006.
- Tian, J. and Chen, D. M.: A semi-empirical model for predicting hourly ground-level fine particulate matter (PM_{2.5}) concentration in southern Ontario from satellite remote sensing and ground-based meteorological measurements, *Remote Sens. Environ.*, 114, 221–229, <https://doi.org/10.1016/j.rse.2009.09.011>, 2010.
- Wang, Z. S., Li, Y. T., Chen, T., Li, L. J., Liu, B. X., Zhang, D. W., Sun, F., Wei, Q., Jiang, L., and Pan, L. B.: Changes in atmospheric composition during the 2014 APEC conference in Beijing, *J. Geophys. Res.*, 120, 12695–12707, <https://doi.org/10.1002/2015JD023652>, 2015.
- Wen, W., Cheng, S., Chen, X., Wang, G., Li, S., Wang, X., and Liu, X.: Impact of emission control on PM and the chemical composition change in Beijing-Tianjin-Hebei during the APEC summit 2014, *Environ. Sci. Pollut. R.*, 23, 4509–4521, <https://doi.org/10.1007/s11356-015-5379-5>, 2016.
- Wu, Q., Xu, W., and Wang, Z.: The air quality forecast about PM_{2.5} before and during APEC 2014 in Beijing by WRF-CMAQ model system, 17, EGU2015-9322, EGU General Assembly Conference Abstracts, 2015.
- Yanosky, J. D., Paciorek, C. J., Laden, F., Hart, J. E., Puett, R. C., Liao, D. P., and Suh, H. H.: Spatio-temporal modeling of particulate air pollution in the conterminous United States using geographic and meteorological predictors, *Environ. Health.*, 13, 63, <https://doi.org/10.1186/1476-069x-13-63>, 2014.
- You, W., Zang, Z. L., Pan, X. B., Zhang, L. F., and Chen, D.: Estimating PM_{2.5} in Xi'an, China using aerosol optical depth: a comparison between the MODIS and MISR retrieval models, *Sci. Total Environ.*, 505, 1156–1165, <https://doi.org/10.1016/j.scitotenv.2014.11.024>, 2015.
- Zhang, J. P., Zhu, T., Zhang, Q. H., Li, C. C., Shu, H. L., Ying, Y., Dai, Z. P., Wang, X., Liu, X. Y., Liang, A. M., Shen, H. X., and Yi, B. Q.: The impact of circulation patterns on regional transport pathways and air quality over Beijing and its surroundings, *Atmos. Chem. Phys.*, 12, 5031–5053, <https://doi.org/10.5194/acp-12-5031-2012>, 2012.
- Zhang, X. Y., Wang, Y. Q., Lin, W. L., Zhang, Y. M., Zhang, X. C., Gong, S., Zhao, P., Yang, Y. Q., Wang, J. Z., Hou, Q., Zhang, X. L., Che, H. Z., Guo, J. P., and Li, Y.: Changes of atmospheric composition and optical properties over Beijing 2008 Olympic monitoring campaign, *B. Am. Meteorol. Soc.*, 90, 1633, <https://doi.org/10.1175/2009BAMS2804.1>, 2009.
- Zhang, W., Zhu, T., Yang, W., Bai, Z., Sun, Y. L., Xu, Y., Yin, B., and Zhao, X.: Airborne measurements of gas and particle pollutants during CAREBeijing-2008, *Atmos. Chem. Phys.*, 14, 301–316, <https://doi.org/10.5194/acp-14-301-2014>, 2014.